THE JOURNAL OF PHYSICAL CHEMISTRY B

Article

pubs.acs.org/JPCB

Impact of Ionic Liquid Pretreatment Conditions on Cellulose Crystalline Structure Using 1-Ethyl-3-methylimidazolium Acetate

Gang Cheng,[†,‡] Patanjali Varanasi,[†,‡] Rohit Arora,[†] Vitalie Stavila,[‡] Blake A. Simmons,[†,‡] Michael S. Kent,[†,‡] and Seema Singh*[,†,‡]

[†]Joint BioEnergy Institute, Emeryville, California 94608, United States

[‡]Sandia National Laboratories, 7011 East Avenue, Livermore, California 94551, United States

Supporting Information

ABSTRACT: Ionic liquids (ILs) have been shown to affect cellulose crystalline structure in lignocellulosic biomass during pretreatment. A systematic investigation of the swelling and dissolution processes associated with IL pretreatment is needed to better understand cellulose structural transformation. In this work, 3−20 wt % microcrystalline cellulose (Avicel) solutions were treated with 1-ethyl-3-methylimidazolium acetate ([C_2mim][OAc]) and a mixture of [C_2mim][OAc] with the nonsolvent dimethyl sulfoxide (DMSO) at different temperatures. The dissolution process was slowed by decreasing the temperature and increasing cellulose loading, and was further retarded by addition of DMSO, enabling in-depth examination of the intermediate stages of dissolution. Results show that the cellulose I lattice expands and distorts prior to full dissolution in [C_2mim][OAc] and that upon precipitation the former structure leads to a less ordered intermediate structure, whereas fully dissolved cellulose leads to a mixture of cellulose II and amorphous cellulose. Enzymatic hydrolysis was more rapid for the intermediate structure (crystallinity = 0.34) than for cellulose II (crystallinity = 0.54).

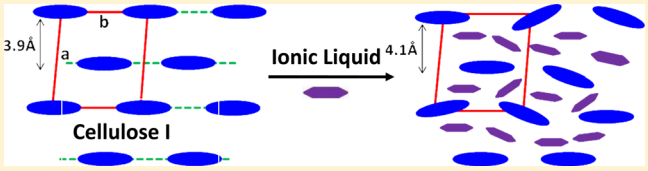

INTRODUCTION

Cellulose is microcrystalline in nature and its native cellulose I structure is recalcitrant to enzymatic hydrolysis.[1−3] In the cellulose I lattice, cellulose chains align in a parallel fashion via hydrogen bonding and van der Waals forces to form a compact and highly ordered microfibril, which consists of crystalline and amorphous regions. Recent progress involving experimental studies and computer simulations have shown that other forms of cellulose such as amorphous cellulose, cellulose II, and cellulose III are less recalcitrant.[3−6] Cellulose II can be obtained from cellulose I via a regeneration process involving dissolution of cellulose in a solvent, followed by precipitation upon addition of an antisolvent such as water.[7] In the cellulose II crystalline form, chains with opposite polarity are stacked to form corrugated sheets. Hydrogen bonding exists within the sheets as well as between them. 1-Ethyl-3-methylimidazolium acetate ([C_2mim][OAc]) has been shown to be one of the most efficient solvents for dissolving cellulose.[8]

The mechanism of dissolution of cellulose in [C_2mim][OAc] and other ionic liquids (ILs) has been studied primarily on a molecular level. It is observed that strong hydrogen bond interactions that occur between [C_2mim][OAc] and cellulose disrupt the intermolecular hydrogen bonds between cellulose molecules.[9,10] In a plant cell wall, however, cellulose chains are arranged in microfibrils that are further aggregated into larger structural units. The supramolecular nature of cellulose requires an understanding of the dissolution mechanism beyond the molecular level, as this would aid in better design and screening of ILs with desired biomass solvation properties. A recent computer simulation study of solvation of a microfibril consisting of 36 glucan chains in 1-butyl-3-methylimidazolium chloride revealed that IL molecules disrupt the interactions between hydrogen-bonded sheets in cellulose I.[5] To capture details of the initial stage of dissolution, it would be much better to study a larger microfibril. However, this would require a less computationally demanding simulation approach or massive computational resources.

Dissolved cellulose molecules in [C_2mim][OAc] form isotropic solutions in dilute solution and self-associate to form liquid crystalline and gel phases at concentrations higher than 10 wt %.[11] Regenerated cellulose has been reported to consist of amorphous cellulose or a mixture of cellulose II and amorphous cellulose.[7,12] The presence of other cell wall components such as lignin further complicates the resulting structures.[13−15] Recrystallization back to cellulose I was observed when biomass samples were treated at lower temperatures with [C_2mim][OAc].[14] While a mechanistic understanding of the interplay between cellulose, lignin, and ionic liquid is still lacking, a systematic study of the impact of a wide range of pretreatment conditions on cellulose crystalline structure would provide important further insight. In this work, [C_2mim][OAc] was used to treat microcrystalline (Avicel) under different conditions. X-ray diffraction (XRD) was used to characterize the crystal structure of the regenerated product.

Received: May 10, 2012
Revised: July 19, 2012
Published: July 23, 2012

ACS Publications © 2012 American Chemical Society

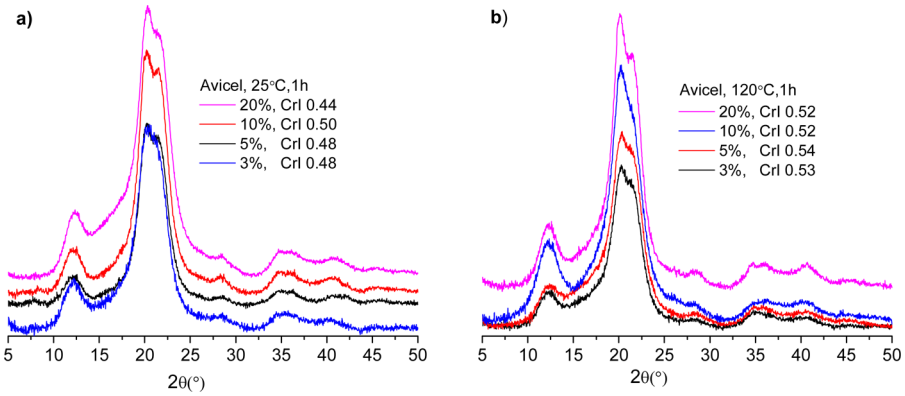

Figure 1. Powder XRD patterns of Avicel treated in [C_2mim][OAc] at (a) 25 °C and (b) 120 °C for 1 h.

The cellulose concentration in [C_2mim][OAc] was varied from 3 to 20 wt %, and the temperature was varied from 0 to 120 °C. In addition to pure [C_2mim][OAc], DMSO was used as a cosolvent to control cellulose solubility, with the aim of revealing intermediate structures during dissolution.

Intermediate structures during the dissolution process were not measured directly in this work but were inferred from measurements of structures that resulted after introduction of a nonsolvent (water) and cellulose precipitation. Introduction of water arrests the dissolution process thereby kinetically trapping intermediate stages, yet it will in some cases further alter the cellulose structure. Using this method, and retarding the dissolution process by varying temperature, cellulose concentration, and solvent composition, intermediate stages and structures in the dissolution process were established. The present approach differs from the approach of a prior study where time-resolved XRD at a synchrotron source was used to directly measure intermediate structures during dissolution.[14]

MATERIALS AND METHODS

Sample Preparation. Measured amounts of as-received Avicel (PH101, Sigma Aldrich) were mixed with 1-ethyl-3-methylimidazolium acetate (90%, Sigma Aldrich), and the mixture was incubated at different temperatures without agitation for specified times. After incubation, hot water was added to the solution to precipitate the dissolved cellulose and the regenerated cellulose was washed extensively with hot water to remove the IL. It was then lyophilized prior to further analysis. After [C_2mim][OAc] pretreatment, samples that were dried under vacuum or at ambient conditions turned yellow (Figure S1 Supporting Information). On the other hand, lyophilization preserved the morphology and color. However, despite the differences in appearance, the crystal structure of samples dried under these different conditions remained the same (Figure S2 in the Supporting Information).

XRD Measurements. Powder X-ray diffraction (XRD) measurements were performed on a PANalytical Empyrean system equipped with a PIXcel^{3D} detector. The Bragg–Brentano geometry comprises a Cu X-ray tube (operated at 45 kV and 40 mA; λ = 1.5418 Å), incident beam optics with a 1/8° fixed divergence, and a 1/4° antiscatter slit as well as a 0.04 rad soller slit and receiving optics which include another 0.04 rad soller slit, a Ni Kβ filter, and the PIXcel^{3D} detector in scanning mode. A reflection–transmission spinner was used as a sample holder and the spinning rate was set at 8 rpm throughout the experiment. The patterns were collected in the 2θ range of 5–65° with a step size of 0.026° and an exposure time of 300 s.

Porosimetry Measurements. Porosimetry measurements were conducted using Micromeritics ASAP 2020 (Norcross, GA). Approximately 500 mg of the sample was degassed for 15 h at 30 °C until a final vacuum of 2 μTorr was reached. The sample was then analyzed for total surface area, pore volume, and pore size distribution using nitrogen porosimetry as described elsewhere.[2] The sample was cooled using liquid nitrogen and dosed with nitrogen gas that condensed on the surface of the pores. Each measurement was taken with a minimum equilibrium time of 100 s to ensure the pressure in the sample chamber had stabilized. The change in the pressure due to condensation was measured. The volume of the nitrogen condensed on the surface was then calculated using Langmuir and Brunauer–Emmett–Teller (BET) models.[16] The pore volume and diameter were calculated based on the BJH (Barrett, Joyner, and Halend) method.[16]

Enzymatic Saccharification. Enzymatic saccharification of untreated and pretreated Avicel samples was conducted at 55 °C and 150 rpm in a 50 mM sodium acetate buffer (pH of 4.8). 50 mg of pretreated Avicel was added to 10 mL of the sodium acetate buffer. CTec2 (Novozymes) was used to conduct enzymatic saccharification. Enzyme loading was maintained at 40 mg of enzyme/g of glucan. The protein concentration of CTec2 was 188 mg/mL. Saccharification reactions were monitored by taking 60 μL of the saccharification supernatant at specific time intervals (0, 0.5, 1, 3, 6, 24, 48, and 72 h).

DNS (3,5-Dinitrosalicylic Acid) Assay. The collected samples were centrifuged at 10 000 g for 5 min, and reducing sugars released during the saccharification were measured by DNS assay. Solutions (0–5 mM) of D-glucose in water were used as calibration standards. The samples collected at 0, 0.5, and 1 h time intervals were diluted by a factor of 5 with water before the addition of DNS. As the samples collected at other time intervals had higher glucose concentration, they were diluted by a factor of 10 with water prior to DNS assay. Error bars show the standard deviation of triplicate measurements.

RESULTS AND DISCUSSION

Parts a and b of Figure 1 show XRD scans of recovered cellulose following incubation in [C_2mim][OAc] for 1 h at 25 and 120 °C, respectively. [C_2mim][OAc] was observed to dissolve up to 20 wt % cellulose at 25 °C. The crystallinity of cellulose II in the recovered cellulose, as indicated in Figure 1, is independent of concentration over the range from 3 to 20 wt % at either temperature. The crystallinity was calculated based

dx.doi.org/10.1021/jp304538v | J. Phys. Chem. B 2012, 116, 10049–10054

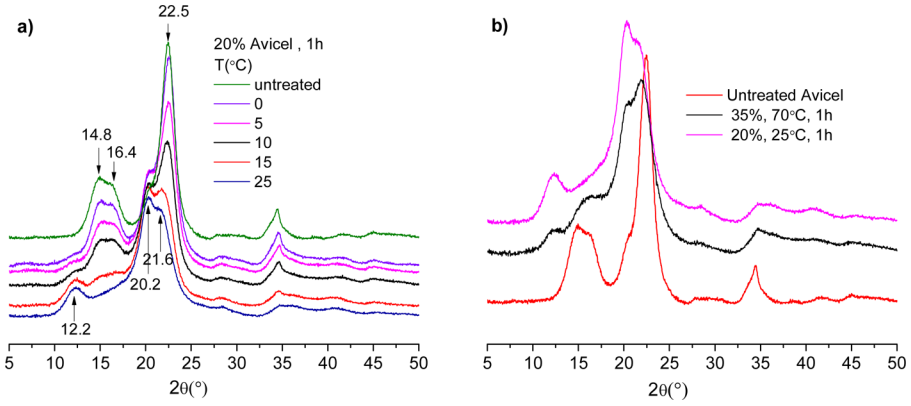

Figure 2. Powder XRD patterns of 20 wt % Avicel treated in $[C_2mim][OAc]$ at temperatures from 0 to 25 °C for 1 h (a), and 35 wt % Avicel treated in $[C_2mim][OAc]$ at 70 °C for 1 h (b).

on the ratio of the area of the crystalline peaks to that of an amorphous cellulose standard (Figure S3 in the Supporting Information).[7] The amorphous cellulose standard was obtained by treatment of Avicel with phosphoric acid.[17] For the samples held at 120 °C, the crystallinity was slightly higher than those treated at 25 °C. This could be due to depolymerization of cellulose, as smaller molecules crystallize more readily. However, this small difference could also result from cellulose existing in different phase states in solution prior to precipitation. On the basis of the phase diagram of cellulose in $[C_2mim][OAc]$, a 20% solution at 120 °C is in a liquid crystalline phase, but transforms to a gel phase at temperatures lower than 100 °C.[11] We note that during the pretreatment, hot water (~85 °C) was added to the solution while it was cooling down from 120 °C. Hot water was used to efficiently remove $[C_2mim][OAc]$. The results shown in Figure 1 demonstrate that the existence of cellulose in either gel or liquid crystalline phases prior to precipitation did not strongly affect the recrystallization to cellulose II.

Several prior studies have reported recrystallization to cellulose I rather than cellulose II following IL pretreatment. A combined autofluorescence microscopy, Raman microscopy, and microprobe XRD investigation on the swelling of the cell wall from lumen at room temperature showed that the solubilized cellulose chains recrystallized to cellulose I. It was proposed that the antiparallel arrangement of cellulose chains could not be achieved in that case due to spatial constraints imposed by intact middle lamella.[15] Recrystallization to cellulose I was also reported in another study of IL treatment of switchgrass, corn stover, and poplar at 50 °C.[14] It was suggested that an intermediate structure was formed where IL molecules intercalated between the cellulose fibers, and that upon washing and drying the cellulose chains recrystallized to cellulose I. Constraints due to the presence of lignin may again have played a role in limiting the extent of dissolution.

To better understand the dissolution and recrystallization processes, we retarded the dissolution process by reducing the temperature so that intermediate structures could be detected. $[C_2mim][OAc]$ readily dissolves cellulose at 20 wt % at room temperature. Figure 2a presents XRD scans of recovered cellulose after incubation in $[C_2mim][OAc]$ at temperatures from 0 to 25 °C for 1 h. A gradual transition from cellulose I to II was observed with increasing treatment temperature. A small shoulder around 12.1° is observable at 0 °C and becomes more pronounced at 5 °C, indicating that a fraction of cellulose transformed into cellulose II. At 25 °C, the broad peaks near 16° disappear, indicating that the dominant phase is cellulose II. The main peak of cellulose I at around 22.5°, corresponding to the distance between hydrogen-bonded sheets, remains roughly at the same position with increasing temperature up to 10 °C. Its intensity as well those of the peaks at 14.8° and 16.4° decrease with increasing treatment temperature, indicating a decreasing amount of cellulose I in the recovered material. This phenomena was seen previously in a study of maple wood flour treated in mixtures of water with $[C_4mim][OAc]$ and $[C_2mim][OAc]$, though it was not discussed in that study.[18] The two peaks at 14.8° and 16.4° are related to intermolecular hydrogen bonds. At 15 °C, the peak at 12.2° clearly indicates the presence of cellulose II, while the peaks at 20.2° and 21.8° could be due to cellulose II or to a mixture of cellulose II and another structure. The existence of an additional structure (as a result of distortion of cellulose I) is suggested by the broad shoulder peak at ~16°, which is reminiscent of cellulose I. The shift of the main peak of cellulose I from 22.5° (d = 3.9 Å) to 21.8° (d = 4.1 Å) indicates an expansion of the lattice, and the reduction of the peaks at 14.8° and 16.4° to a weak shoulder peak suggests a disturbance of the arrangement of cellulose chains within the hydrogen-bonded sheets. We propose that the cellulose chains within one hydrogen-bonded sheet are almost amorphous while the orientational order perpendicular to the sheets still persists, a structure similar to a nematic liquid crystal. The results show that the original cellulose I lattice was distorted and transformed into a less ordered intermediate structure. Further evidence of this intermediate structure will be presented below.

The slight increase of the intersheet distance is likely caused by the insertion of IL molecules, leading to an expansion of the cellulose I lattice. We speculate that the IL molecules diffuse into the gap between the hydrogen-bonded sheets. Evidence for this was reported recently in molecular dynamics simulations[19] Upon subsequent washing by water, these IL molecules are washed away while the expanded lattice structure remains. A prior XRD study of *Cladophora* cellulose under heat treatment recorded a 6% expansion of the intersheet distance, which is similar to our result.[20] Schematic illustrations of the cellulose I structure and the proposed $[C_2mim][OAc]$-induced distorted structure are shown in Figure 3, a and b, respectively.

The structure that we propose here for $[C_2mim][OAc]$-treated Avicel is quite different from structures proposed in prior studies. In a prior molecular dynamics study of cellulose II regeneration in water, a sheetlike structure was initially formed where glucopyranose rings were stacked by hydrophobic

dx.doi.org/10.1021/jp304538v | J. Phys. Chem. B 2012, 116, 10049−10054

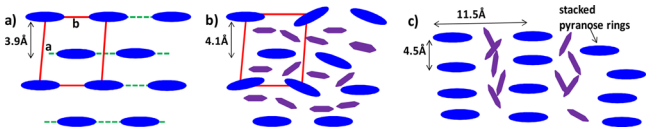

Figure 3. (a) Schematic representation of cellulose chain (blue) arrangement for the view parallel to the chain *c* axis and the unit cell for cellulose I_β. The dotted lines along the *b* axis represent the intermolecular hydrogen bonding that forms sheet structure. (b) The intermediate structure and the intercalation of [C_2mim][OAc] molecules (purple) proposed here. (c) Proposed intermediate structure and the arrangement of intercalated [C_2mim][OAc] molecules in ramie fibers from Samayam et al.[14]

interactions.[21] In that case, the cellulose chains were fully dissolved before regeneration. Later, those stacks of chains (sheets) associated with each other by hydrogen bonds to form lamellar structures. A recent fiber XRD investigation on ramie fiber swollen with [C_2mim][OAc] suggested that IL molecules were intercalated between the stacks.[14] The distance between the stacks swollen with IL was 11.5 Å and the distance between glucopyranose rings was 4.5 Å.[14] Avicel powder treated under the same conditions did not show this intermediate structure and transformed to cellulose II upon regeneration. This lamellar structure, defined by a characteristic length of 11.5 Å, corresponds to a 2θ of 7.7° for a wavelength of 1.54 Å. This peak was not observed in the XRD data of the current work, where Avicel powder was used.

Coexistence of cellulose II with the intermediate structure was also observed when 35 wt % Avicel was added to the [C_2mim][OAc] and the solution was incubated at 70 °C for 1 h (Figure 2b). For each case we propose that the increased viscosity of the solution dramatically slowed down ion diffusion,[17] prolonging the transition state involving a mixture of both expanded cellulose I and dissolved cellulose. Upon expulsion of [C_2mim][OAc] from the swollen cellulose I lattice with water, the intermediate structure was produced whereas cellulose II was formed from the dissolved cellulose. This is different from the above-mentioned study where recrystallization back to the undistorted cellulose I was observed.[14]

The intermediate structure proposed here represents a structure that is kinetically frozen upon addition of water into cellulose/[C_2mim][OAc] mixtures during the process of dissolution. A computer simulation study of cellulose microfibrils in 1-butyl-3-methylimidazolium chloride also suggested that both the cation and anion disturb the intersheet interactions, consistent with an expanded lattice transition structure.[5]

Generation of the intermediate structure upon precipitation requires that [C_2mim][OAc] only swell, but not completely dissolve, the cellulose crystalline structure. A weaker solvating power can be achieved by mixing [C_2mim][OAc] with DMSO, a nonsolvent for cellulose. Figure 4a presents XRD data of recovered cellulose after incubation in [C_2mim][OAc]/DMSO (10/90 by wt) at 120 °C for 1 h and subsequent precipitation. For a 20 wt % solution, the cellulose I structure remained intact after the treatment. However, with decreasing cellulose concentration the intermediate structure was generated upon precipitation. The large full width at half-maximum (fwhm) of the observed diffraction peaks indicates a partial loss of long-range order. For the 10 and 5 wt % solutions, the treatment did not lead to cellulose II, indicating the absence of full dissolution. For the 3 wt % solution, a weak shoulder peak

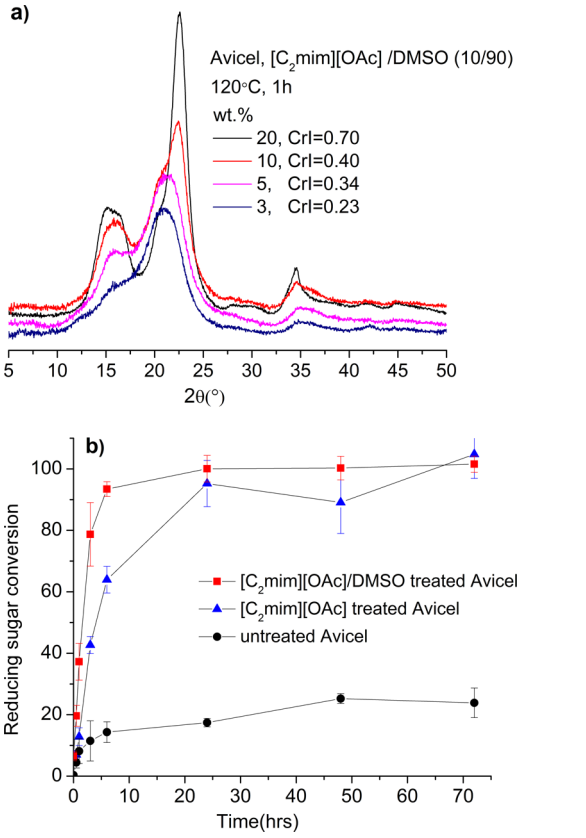

Figure 4. (a) Powder XRD patterns of 3, 5, 10, and 20 wt % Avicel treated in a DMSO/[C_2mim][OAc] mixed solvent (90 wt % DMSO, 10 wt % [C_2mim][OAc]) at 120 °C for 1 h. (b) Saccharification data of untreated, [C_2mim][OAc], and DMSO/[C_2mim][OAc] mixed solvent treated Avicel at 5 wt % loading.

appears at 12.5° after the treatment, indicating that a small amount of dissolution occurred resulting in cellulose II formation upon precipitation. The spectra in Figure 4 indicate the presence of an expanded cellulose I lattice along with greatly increased amorphous content. These observations are consistent with greater ion mobility and more intercalation of the ions into the lattice at lower cellulose concentrations, as mentioned above, along with the decreased solvating power of the cosolvent. For comparison, 5 wt % cellulose in [C_2mim]-[OAc] /DMSO(10/90) is equivalent to 34 wt % cellulose in 100% [C_2mim][OAc] based solely on the ratio of cellulose to [C_2mim][OAc]. The fact that no cellulose II was observed at 5 wt % cellulose incubated for 1 h at 120 °C in [C_2mim][OAc] /DMSO (10/90) whereas cellulose II was clearly detected for 35 wt % cellulose incubated for 1 h in 100% [C_2mim][OAc] at 70 °C is consistent with the fact that that DMSO suppresses the solubility of [C_2mim][OAc].

Results for the saccharification of [C_2mim][OAc] and [C_2mim][OAc]/DMSO-treated Avicel are compared in Figure 4b along with results for untreated Avicel. Avicel samples were treated at 5 wt % loading. Both the initial hydrolysis rate and the overall conversion for treated Avicel are far greater than those of untreated Avicel. This is due to disruption of the native cellulose I structure and weaker intersheet interactions. Prior studies suggested that intersheet interactions are the main cause of cellulose recalcitrance.[22] The initial hydrolysis rate for Avicel treated in [C_2mim][OAc]/DMSO(10/90) was noticeably greater than that for Avicel treated in [C_2mim][OAc]. The

dx.doi.org/10.1021/jp304538v | J. Phys. Chem. B 2012, 116, 10049−10054

Table 1. Porosimetry Measurement of 5% Avicel Pretreated in [C_2mim][OAc] and in the [C_2mim][OAc]/DMSO Mixed Solvent

	surface area (m^2/g)		surface area (m^2/g) (for pores between 17.000 and 3000.000 Å dia)		pore volume (cm^3/g) × 10^{-3} (for pores between 17.000 and 3000.000 Å dia)	
	BET	Langmuir	BJH adsorpn	BJH desorpn	BJH adsorpn	BJH desorpn
untreated	0.95 ± 0.03	1.38 ± 0.04	0.63 ± 0.07	0.61 ± 0.06	3.18 ± 0.02	2.34 ± 0.01
IL	3.44 ± 0.03	5.14 ± 0.05	3.38 ± 0.04	2.88 ± 0.01	12.32 ± 0.18	9.68 ± 0.11
IL/DMSO	8.4 ± 0.04	12.38 ± 0.07	7.79 ± 0.07	7.1 ± 0.01	30.29 ± 2.54	26.37 ± 1.67

surface area of cellulose (Table 1) increased by a factor of 4 after [C_2mim][OAc] treatment and by a factor of 10 after [C_2mim][OAc]/DMSO treatment, which correlates with the improved hydrolysis efficiencies. It is noted that the CrI of cellulose II was 0.54 after the [C_2mim][OAc] treatment and that of distorted cellulose I was 0.34. Although obtaining a detailed understanding of the relative reactivity of cellulose II and the intermediate structure is beyond the scope of the present work, it is certain that greater amorphous cellulose content and surface area play important roles in the increased hydrolysis efficiency.

CONCLUSION

The structural rearrangement of microcrystalline cellulose during [C_2mim][OAc] treatment and regeneration by precipitation was studied by powder XRD. As the dissolution process progressed, the order of the cellulose I structure in the regenerated material decreased. The XRD data suggests that during dissolution [C_2mim][OAc] molecules penetrate into the gap between hydrogen-bonded sheets in cellulose I and cause a slight expansion of the lattice. Concurrently, intermolecular hydrogen bonds are disturbed such that the long-range order within each sheet decreases. The rate of the dissolution process was slowed by decreasing the temperature and also by increasing the cellulose loading. This resulted in the observation of an intermediate structure along with cellulose II. We propose that upon precipitation the intermediate structure forms from the material with the distorted cellulose I lattice whereas cellulose II forms from fully dissolved cellulose. In each case, amorphous cellulose was also produced. The dissolution process was also retarded by using a mixture of [C_2mim][OAc] and the nonsolvent DMSO. For this cosolvent system, upon precipitation the intermediate structure was isolated with little or no cellulose II formation. Saccharification data indicated more rapid digestion of the less ordered intermediate structure with a CrI of 0.34, formed by treatment of 5 wt % Avicel with the 10%/90% [C_2mim][OAc]/DMSO mixture, than that of cellulose II with a CrI of 0.54 resulting from treatment with 100% [C_2mim][OAc].

ASSOCIATED CONTENT

Supporting Information

Photos of regenerated cellulose dried under vacuum or at ambient conditions and using a lyophilizer (Figure S1). XRD patterns of regenerated cellulose dried under vacuum, at ambient conditions and using a lyophilizer (Figure S2). Estimation of cellulose CrI by comparing area of XRD curves (Figure S3). This material is available free of charge via the Internet at http://pubs.acs.org.

AUTHOR INFORMATION

Notes

The authors declare no competing financial interest.

ACKNOWLEDGMENTS

This work was part of the DOE Joint BioEnergy Institute (http://www.jbei.org) supported by the U.S. Department of Energy, Office of Science, Office of Biological and Environmental Research, through contract DE-AC02-05CH11231 between Lawrence Berkeley National Laboratory and the U.S. Department of Energy.

REFERENCES

(1) Chundawat, S. P. S.; Donohoe, B. S.; da Costa Sousa, L.; Elder, T.; Agarwal, U. P.; Lu, F.; Ralph, J.; Himmel, M. E.; Balan, V.; Dale, B. E. *Energy Environ. Sci.* **2011**, *4*.
(2) Li, C. L.; Cheng, G.; Balan, V.; Kent, M. S.; Ong, M.; Chundawat, S. P. S.; Sousa, L. D.; Melnichenko, Y. B.; Dale, B. E.; Simmons, B. A.; Singh, S. *Bioresour. Technol.* **2011**, *102*, 6928.
(3) Chundawat, S. P. S.; Bellesia, G.; Uppugundla, N.; Sousa, L. D.; Gao, D. H.; Cheh, A. M.; Agarwal, U. P.; Bianchetti, C. M.; Phillips, G. N.; Langan, P.; Balan, V.; Gnanakaran, S.; Dale, B. E. *J. Am. Chem. Soc.* **2011**, *133*, 11163.
(4) Beckham, G. T.; Matthews, J. F.; Peters, B.; Bomble, Y. J.; Himmel, M. E.; Crowley, M. F. *J. Phys. Chem. B* **2011**, *115*, 4118.
(5) Gross, A. S.; Bell, A. T.; Chu, J. W. *J. Phys. Chem. B* **2011**, *115*, 13433.
(6) Igarashi, K.; Uchihashi, T.; Koivula, A.; Wada, M.; Kimura, S.; Okamoto, T.; Penttila, M.; Ando, T.; Samejima, M. *Science* **2011**, *333*, 1279.
(7) Cheng, G.; Varanasi, P.; Li, C. L.; Liu, H. B.; Menichenko, Y. B.; Simmons, B. A.; Kent, M. S.; Singh, S. *Biomacromolecules* **2011**, *12*, 933.
(8) Zavrel, M.; Bross, D.; Funke, M.; Büchs, J.; Spiess, A. C. *Bioresour. Technol.* **2009**, *100*, 2580.
(9) Liu, H. B.; Sale, K. L.; Holmes, B. M.; Simmons, B. A.; Singh, S. *J. Phys. Chem. B* **2010**, *114*, 4293.
(10) Zhang, J. M.; Zhang, H.; Wu, J.; Zhang, J.; He, J. S.; Xiang, J. F. *Phys. Chem. Chem. Phys.* **2010**, *12*, 1941.
(11) Song, H. Z.; Niu, Y. H.; Wang, Z. G.; Zhang, J. *Biomacromolecules* **2011**, *12*, 1087.
(12) Dadi, A. P.; Varanasi, S.; Schall, C. A. *Biotechnol. Bioeng.* **2006**, *95*, 904.
(13) Wu, H.; Mora-Pale, M.; Miao, J. J.; Doherty, T. V.; Linhardt, R. J.; Dordick, J. S. *Biotechnol. Bioeng.* **2011**, *108*, 2865.
(14) Samayam, I. P.; Hanson, B. L.; Langan, P.; Schall, C. A. *Biomacromolecules* **2011**, *12*, 3091.
(15) Lucas, M.; Wagner, G. L.; Nishiyama, Y.; Hanson, L.; Samayam, I. P.; Schall, C. A.; Langan, P.; Rector, K. D. *Bioresour. Technol.* **2011**, *102*, 4518.
(16) Barrett, E. P.; Joyner, L. G.; Halenda, P. P. *J. Am. Chem. Soc.* **1951**, *73*, 373.
(17) Bansal, P.; Hall, M.; Realff, M. J.; Lee, J. H.; Bommarius, A. S. *Bioresour. Technol.* **2010**, *101*, 4461.
(18) Doherty, T. V.; Mora-Pale, M.; Foley, S. E.; Linhardt, R. J.; Dordick, J. S. *Green Chem.* **2010**, *12*.
(19) Liu, H.; Cheng, G.; Kent, M. S.; Stavila, V.; Simmons, B. A.; Sale, K. L.; Singh, S. *J. Phys. Chem. B* **2012**.
(20) Wada, M.; Kondo, T.; Okano, T. *Polym. J.* **2003**, *35*, 155.
(21) Miyamoto, H.; Umemura, M.; Aoyagi, T.; Yamane, C.; Ueda, K.; Takahashi, K. *Carbohydr. Res.* **2009**, *344*, 1085.

(22) Cho, H. M.; Gross, A. S.; Chu, J. W. *J. Am. Chem. Soc.* **2011**, *133*, 14033.